Full characterisation of a background limited antenna coupled KID over an octave of bandwidth for THz radiation

Bueno, J.; Yurduseven, O.; Yates, S.J.C.; Llombart, N.; Murugesan, V.; Thoen, D.J.; Baryshev, A.M.; Neto, A.; Baselmans, J.J.A.

Important note
To cite this publication, please use the final published version (if applicable).
Please check the document version above.

Full characterisation of a background limited antenna coupled KID over an octave of bandwidth for THz radiation

J. Bueno,[1,a)] O. Yurduseven,[2] S. J. C. Yates,[3] N. Llombart,[2] V. Murugesan,[1] D. J. Thoen,[2] A. M. Baryshev,[3,4] A. Neto,[2] and J. J. A. Baselmans[1,2]

[1]*SRON - Netherlands Institute for Space Research, Sorbonnelaan 2, 3584 CA Utrecht, The Netherlands*
[2]*Department of Microelectronics, Faculty of Electrical Engineering, Mathematics and Computer Science (EEMCS), Delft University of Technology, Mekelweg 4, 2628 CD Delft, The Netherlands*
[3]*SRON - Netherlands Institute for Space Research, Landleven 12, 9747 AD Groningen, The Netherlands*
[4]*Kapteyn Astronomical Institute, University of Groningen, Landleven 12, 9747 AD Groningen, The Netherlands*

We present the design, fabrication, and full characterisation (sensitivity, beam pattern, and frequency response) of a background limited broadband antenna coupled kinetic inductance detector covering the frequency range from 1.4 to 2.8 THz. This device shows photon noise limited performance with a noise equivalent power of 2.5×10^{-19} W/Hz$^{1/2}$ at 1.55 THz and can be easily scaled to a kilo-pixel array. The measured optical efficiency, beam pattern, and antenna frequency response match very well the simulations. © 2017 Author(s). All article content, except where otherwise noted, is licensed under a Creative Commons Attribution (CC BY) license (http://creativecommons.org/licenses/by/4.0/). [http://dx.doi.org/10.1063/1.4985060]

The next generation of space based imaging spectrometers for sub-millimeter (sub-mm) wave astronomy requires broad band radiation coupling between 1 and 10 THz.[1,2] These spectrometers will allow measurements of a large number of spectroscopic bands over a wide area of the sky in a very limited time. In order to do so, they will require a large number of pixels to cover the telescope field of view or to sample a given frequency band with a high resolution. Kinetic Inductance Detectors (KIDs) are superconducting pair-breaking resonators[3] that are a very attractive choice for these applications since thousands of detectors can be read-out with a single coaxial feed line,[3–5] enabling simple and cost-effective systems.

Broad band radiation coupling to KIDs can be achieved by using Lumped Element Kinetic Inductance Detectors (LEKIDs),[6] where the radiation is coupled to the inductive section of a resonator, or by coupling planar[7] or horn[8] antennas to the inductive section of the KID. Niobium (Nb) and niobium titanium nitride (NbTiN) technology allows the on-chip fabrication of lossless superconducting striplines and filters between the antenna and the KIDs. At frequencies exceeding the gap frequency (650 GHz for Nb and 1.1 THz for NbTiN), ohmic losses will make this technology impractical. Radiation detection using antennas is still possible, but antenna and KID must be integrated into a single structure to prevent signal loss between them.[9,10] Additionally, these high frequencies are only accessible from space, which results in very high requirements on the detector sensitivity,[12] typically with an noise equivalent power (NEP) of $\sim 3 \times 10^{-19}$ W/Hz$^{1/2}$ for a non-dispersive spectrometer. Such sensitivities and photon noise performance are achieved with antenna coupled aluminium (Al) KIDs over a broad band[9] around 1.5 THz with poor beam quality and over a narrow band around 850 GHz.[5,11] In this paper, we extend KID technology to higher frequencies and large bandwidths using a leaky lens antenna coupled device.

We intend to make a detector that can be used in an imaging spectrometer, such as the SPICA-SAFARI concept presented by Roelfsma et al.[1] A reasonable set of detector requirements is: (i) Frequency band coverage over an octave at a frequency higher than 1 THz; (ii) radiation detection in 2 polarisations; (iii) antenna scalable between 1 and 10 THz using a reliable fabrication technique over large areas (minimum dimension $\sim$100 nm); and (iv) detector aperture efficiency larger than 50%. The aperture efficiency η_{ap} is defined as the ratio between the effective area and the physical area of the lens antenna. For this paper, we have chosen to cover the low frequency band (1.4 − 2.8 THz) of the SPICA-SAFARI instrument.[1] We also choose to design a single polarisation prototype, as this allows a more straightforward integration with the KID. Coming to a choice for the antenna, we compare printed antennas that have a broad band coverage: the log spiral antenna,[13] the sinuous antenna,[14] and the leaky lens antenna.[15] A compilation with all the expected performance for these antennas can be found in Yurduseven et al.,[16] and it is summarised in Table I. We select the leaky lens antenna because it requires much larger minimum dimensions. At 10 THz, the minimum dimension needed for the spiral and sinuous antennas of $\lambda_0/2000$ requires 15 nm features, which are very difficult to fabricate reliably over a large area.

TABLE I. This table shows the expected performance of the antennas studied in this paper. The lens coupled leaky lens antenna is the only one that meets all the requirements.

	Requirement	Spiral	Sinuous	Leaky lens
Bandwidth	1:2	1:7	1:4	1:2.5
Aperture efficiency	>50%	$\sim$50%	$\sim$40%	$\sim$60%
Polarisation	Dual	Circular	Dual	Dual
Minimum dimension	$>\lambda_0/300^a$	$\lambda_0/2100$ (Ref. 17)	$\lambda_0/2000$ (Ref. 18)	$\lambda_0/100$ (Ref. 16)

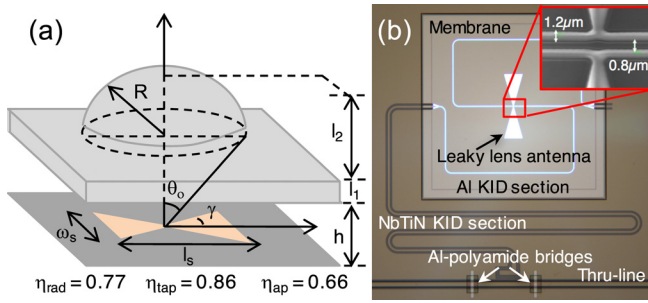^{a}100 nm at 10 THz

a)j.bueno@sron.nl

FIG. 1. (a) Sketch of the optimised slot and lens geometry with their design parameters. (b) Back and front illuminated optical image of a single pixel of the leaky lens antenna coupled KID. The light goes through the membrane where both the antenna and the Al section of the KID are fabricated. The centre of the antenna is shown with an SEM image.

The leaky lens antenna[15] is a lens feed consisting of a leaky wave slot kept at an electrically small distance from the dielectric lens in order to obtain a highly directive radiation pattern inside the dielectric. Consequently, it efficiently illuminates the lens. This has been proved experimentally at lower frequencies.[19] Our current design, shown in Fig. 1(a), is optimised to obtain a high, frequency independent, aperture efficiency over the entire bandwidth between 1.4 and 2.8 THz. The optimisation of the slot yields a slot width $w_s = 173\,\mu m$, slot length $l_s = 602\,\mu m$, slot tapering angle $\gamma = 15°$, and the air-gap between the antenna and the silicon lens $h = 3\,\mu m$. The lens is optimised obtaining a lens slab $l_1 = 737\,\mu m$, a lens height $l_2 = 442\,\mu m$, a subtended angle $\theta_0 = 46.5°$, and radius of the lens $R = 900\,\mu m$. The generic parameter that describes the lens-antenna efficiency is the aperture efficiency $\eta_{ap} = \eta_{rad} \times \eta_{tap}$. Here, η_{rad} is the radiation efficiency, defined as the fraction of the power absorbed by the central conductor of the coplanar waveguide (CPW) line in the KID, and η_{tap} is the taper efficiency, which relates to the illumination of the lens. A detailed explanation of these efficiencies in antenna coupled KIDs can be found in Ferrari *et al.*[11] We find $\eta_{rad} = 0.77$, $\eta_{tap} = 0.86$, and $\eta_{ap} = 0.66$ for our design.

The KID is designed, combining the hybrid NbTiN/Al technology,[20] the all-Al antenna concept,[9] and the leaky lens antenna printed on a thin SiN membrane.[19] The NbTiN-Al hybrid KID, due to the reduction in KID internal two level systems (TLS) noise[21] by the use of NbTiN,[22] allows multiplexing of thousands of KIDs with phase readout.[4] The

all-aluminium antenna concept is used because a NbTiN ground plane would result in very significant signal loss in the antenna ground plane at frequencies above the NbTiN superconducting gap ($\sim$1.1 THz for a T_c of $\sim$15 K). The all-Al antenna concept uses a thick 100 nm ground plane and a thin 50 nm central KID strip.[9] The Al has a lower resistivity than the NbTiN. Hence, a thick Al ground plane yields a lower loss above 1.1 THz, resulting in an absorption of the THz radiation to the central strip of the KID of $\sim$90%.

A front and back illuminated optical image of the leaky lens coupled KID is shown in Fig. 1(b). The KID is a section of coplanar waveguide (CPW), shorted at its far end and open ended near the feedline. The KID length is $\sim$8 mm, corresponding with a resonant frequency of $\sim$3.5 GHz. THz radiation is coupled to the slot in the Al ground plane, which launches the radiation into the two, very narrow, Al CPW lines. The length of the Al lines ($\sim$1.25 mm) is such that all THz radiation is absorbed before the lines become wide. The narrow linewidth (0.8 μm strip with a 1.2 μm gap) is needed to limit radiation loss. The narrow Al line broadens at either end and connects to a wide NbTiN CPW. The NbTiN central conductor is shorted to the NbTiN ground at the far end of the resonator. At the other end, the NbTiN that remains wide (strip of 12 μm with a gap of 8 μm) is deposited on the bare Si substrate for most of its length. Both strategies reduce the TLS noise[23] so photon noise can be observed using the phase signal readout.

We fabricate a 19 pixel array, hexagonally packed, with a pitch of 1.6 mm. The fabrication process starts with a 375 μm thick high resistivity ($>$10 kΩ cm) $\langle 100 \rangle$ orientation Si wafer, covered with a low tensile stress ($\sim$250 MPa) low pressure chemical vapour deposited (LPCVD) SiN with a thickness of 1 μm on both sides [Fig. 2(a-1)]. The SiN on the back of the wafer is etched with reactive ion etching (RIE) to define the future location of the SiN frontside membrane. We use RIE using 35% SF$_6$ and 65% O$_2$ to create a sloped edge on the front SiN, etching the SiN everywhere except where the membrane will be [Fig. 2(a-2)]. We deposit a 350 nm thick layer of NbTiN using reactive sputtering of a NbTi target (81.9% Nb and 18.1% Ti, with a purity 99.95%) in an Ar/N$_2$-rich atmosphere on the front side of the wafer [Fig. 2(a-3)]. The SiN sloped edge allows a good step coverage of the NbTiN layer. The NbTiN is patterned defining the wide section of the KID resonator, the transmission line connecting
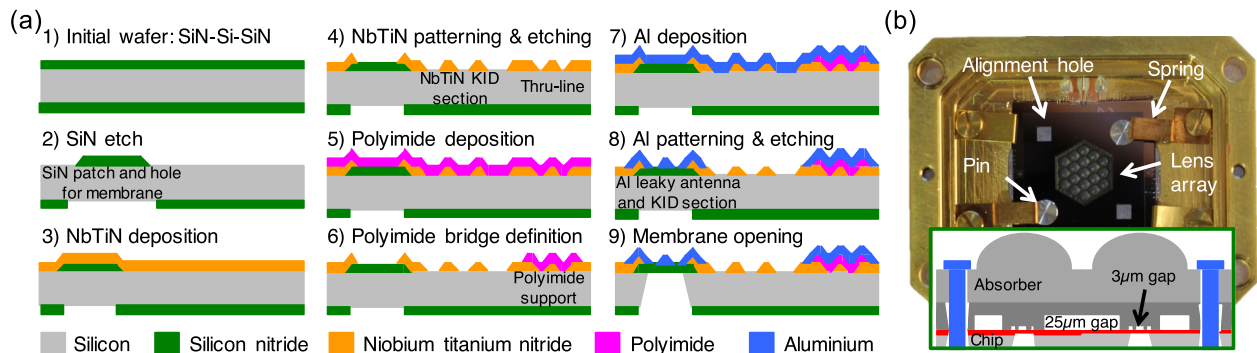

FIG. 2. (a) Schematic drawing (not to scale) of the process flow. A detailed description of the fabrication process can be found in the text. (b) Picture and schematic drawing of the antenna-KID chip, spacer, and lens array assembly. The KID and antenna are fabricated on a membrane, a spacer wafer is placed on top of it to assure the 3 μm gap, and the lens goes on top of them.

all detectors and a large square aperture almost as large as the membrane [Fig. 2(a-4)]. We use the same reactive ion etching process to create a sloped edge on the NbTiN to allow good step coverage for the Al. Next, we spin coat 1 μm polyimide LTC9505 on the wafer [Fig. 2(a-5)]. The photosensitive poly-imide is patterned and cured into a dielectric stub with sloped edges that will give the support of the superconducting short between the ground planes of the feedline[24] [Fig. 2(a-6)]. The wafer is then immersed in a 10% diluted solution of HF for 10 s to remove surface oxides and organic contaminations and guarantee a clean NbTiN-Al interface. Immediately after-wards, a film of Al with a thickness of 75 nm is sputtered on the front side of the wafer [Fig. 2(a-7)], patterned, and wet etched with a commercially available Al etchant[25] [Fig. 2(a-8)]. The thickness of the Al is chosen such that it is thicker than the penetration depth at 1.4 THz to assure radia-tion absorption. It is important that the Al thickness is thicker than the penetration depth to assure that all the THz radiation is absorbed. If the antenna was thinner than the penetration depth, less current would be induced with the consequent reduction in the absorbed power and drop in the coupling effi-ciency. The opening of the membrane is done by submerging the wafer in a KOH bath while protecting the front side of the wafer [Fig. 2(a-9)]. Afterwards, a SC-2 (Standard Clean 2) cleaning step[26] is introduced in order to eliminate potassium residue on the membrane back side. This additional cleaning has proven to enhance the internal Q factor (Q_i) of the resona-tors from 40 to 50 thousand (without the SC-2 clean) up to a few millions and reduce the TLS noise.

To create the 3D structure required for the operation of the leaky lens antenna, we use an assembly of three different chips: the antenna chip, the spacer wafer that assures a 3 μm gap, and the lens array, which is shown in Fig. 2(b). The lens array is made out of a 1 mm thick, >10 kΩ cm, $\langle 100 \rangle$ silicon wafer using laser ablation.[27] The spacer chip is fabricated on a 250 μm thick, >10 kΩ cm, $\langle 100 \rangle$ orientation Si wafer cov-ered with a low tensile stress (~250 MPa) LPCVD SiN with a thickness of 300 nm on both sides. Alignment holes are created with a KOH etch. A 3 μm gap is etched with RIE on the spacer chip at the position where the antennas are placed. A few columns are left on the gap to prevent the membrane of sticking to the spacer chip. A second etch of 25 μm is per-formed, after covering the 3 μm gap, to increase the distance between the chip with the antenna and KIDs and the spacer wafer. This is done in order to minimise the area in which particles larger than 3 μm can be sandwiched in between the two chips. The alignment accuracy achieved with this method is 15 μm.

We measure the device sensitivity and coupling effi-ciency mounting the chip on a sample box inside a light-tight box, in a pulse tube pre-cooled Adiabatic Demagnetization Refrigerator (ADR). The sub-mm calibration signal is sup-plied by a black body radiator whose temperature can be var-ied from 3 up to 35 K. The radiation is coupled to the detector via a series of 8 metal mesh IR filters, defining an optical bandpass of 0.1 THz centred around 1.55 THz.[9] A 2.65 mm diameter aperture is placed at 20 mm of the lens to limit the throughput. The power absorbed from the black body source by the Al strip equals $P_{abs} = 0.5 \eta_{opt} \int \lambda^2 F_\nu B_\nu d\nu$, where the factor 0.5 is associated with a single-polarised antenna, η_{opt} is

the optical coupling efficiency, λ is the wavelength of the incoming radiation, F_ν is the filter frequency response, and B_ν is the mode occupation. The optical coupling efficiency $\eta_{opt} = \eta_{rad} \times \eta_{so}$ describes the fraction of the power emitted from the black body source that is absorbed in the Al strip of the KID, where η_{so} is the spill over efficiency, defined as the ratio of power of the antenna beam that is contained in the solid angle defined by the limiting aperture to the black body source with respect to the total beam power.

We have made some design choices to ease the fabrica-tion and assembly of the device: (i) The lens array does not have an anti-reflective coating to probe the broad band recep-tion, introducing an ~30% reflection loss. (ii) The Al section of the KID and the antenna ground plane are made of a sin-gle layer, resulting in ~30% of the power coupled to the antenna to be absorbed in the ground plane; and (iii) the Al CPW has a total width of 3.2 μm, limited by the resolution of the optical lithography, with an impedance mismatch to the antenna and a radiation loss of ~9% and ~6%, respec-tively. The combined effect is a reduction of η_{rad} to 0.37. Additionally, we found that the lens array is misaligned with respect to the antenna position by 15 μm, which reduces the spill over efficiency η_{so} from 0.45 (for a well aligned system) to 0.3. The expected optical coupling efficiency between the KID and the black body radiator $\eta_{opt} = \eta_{rad} \times \eta_{so} = 0.11$. The effective implementation strategy chosen leads to an aperture efficiency $\eta_{ap} = \eta_{rad} \times \eta_{tap} = 0.24$.

We measure first the device noise at a temperature T = 120 mK and a black body radiator temperature of 3 K. The internal quality factor Q_i is ~2×10^6, and the loaded quality factor Q is ~50×10^3. At this temperature, the power emitted by the radiator in the frequency band defined by the filters is negligible. The measured noise under these condi-tions is shown in Fig. 3(a) as the solid dark blue line. The black line represents an estimation of the TLS-dominated device noise, obtained from two measured reference resona-tors (wide NbTiN resonator and narrow Al resonator) and the assumption of a $|\vec{E}|^3$-TLS noise dependence.[23,28] As the black body source temperature increases, the power spectral density also increases, and eventually, the noise level becomes flat and remains constant. Moreover, the roll-off between 0.1 and 1 kHz (due to the quasiparticle lifetime) is reduced by an increasing optical load following a $P_{source}^{-1/2}$ dependence. We thus conclude that the device is photon noise limited at absorbed powers $P_{abs} > 1$ fW.

To measure the NEP and coupling efficiency of the detector, we use the method developed by Ferrari *et al.*[11] The measured NEP is given by $NEP^2(\omega) = S_\theta(\omega)/(\delta\theta/\delta P_{abs})^2$, where S_θ is the power spectral density of the phase signal and $\delta\theta/\delta P_{abs}$ is the phase responsivity. We measure an optical NEP equal to 2.5×10^{-19} W/Hz$^{1/2}$ at the lowest load-ing and is shown in Fig. 3(b). The background limited NEP equals $NEP_{BLIP} = \sqrt{2h\nu P_{abs}(1 + \eta_{opt}F_\nu B_\nu) + 4\Delta P_{abs}/\eta_{pb}}$, in which h is Planck's constant, ν is the radiation frequency, $(1 + \eta_{opt}F_\nu B)$ is the correction to Poissonian statistics due to photon bunching, Δ is the superconducting energy gap, and η_{pb} is the pair breaking efficiency. We observe a good match between the data (dots) and NEP_{BLIP} (calculated). A more
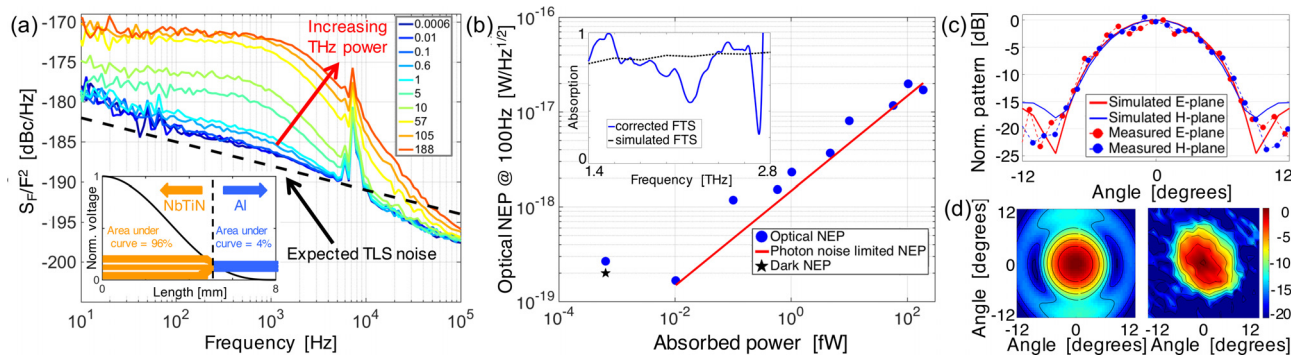
FIG. 3. (a) Power spectral density measured as a function of the absorbed power. The inset is an estimation of the weight of the noise for each section of the KID. (b) Measured dark and optical NEP at a measured frequency of 100 Hz, expected photon noise limited NEP and fit to the optical NEP to obtain the optical efficiency. The inset shows FTS of the leaky lens antenna showing a large frequency range (over an octave of bandwidth), limited by the optical filters in the setup. (c) Main lobe of the leaky lens antenna beam pattern measured at 1.55 THz. (d) Simulated (left) and measured (right) beam pattern of the leaky lens antenna. The side lobes cannot be measured due to the limited field of view of the setup.

detailed analysis[11] of the data results in $\eta_{opt,meas} = 0.106$, which is very close to the calculated value.

To measure the beam pattern and frequency response, we mount the device on the cold stage ($\sim$300 mK) of a He7 cooler with optical access from room temperature with several filters, defining a frequency window from 1 to 2.7 THz. A glow bar with 2 mm diameter aperture acts as the source of radiation. The source is placed outside the cryostat and can be moved using motor controlled translational stages in the two directions orthogonal to the optical axis of the detector beam. A polariser is placed in front of the glow bar. A narrow band pass filter centred at around 1.55 THz in front of the glow bar is added for the beam pattern measurement and removed for frequency response measurement. The source is modulated at a few Hz to remove 1/f noise from the system. The measured pattern at around 1.55 THz is shown in Figs. 3(c) and 3(d) together with the simulated one, showing a good agreement. The elliptical shape of the beam pattern is tentatively attributed to the radiation absorbed by the common mode of the KID CPW close to the antenna. The frequency response of the detector, measured using a Fourier Transform Spectrometer (FTS), is shown in the inset of Fig. 3(b). The FTS shows a frequency range larger than an octave of bandwidth, limited by the optical filters in the setup (1 THz and 2.7 THz for the lower and higher frequencies, respectively). In this experiment, we lower the pressure in the entire setup, which reduces but does not eliminate completely the absorption from water. The dip in the frequency response is tentatively attributed to a poor correction for water absorption lines.

We have fabricated and tested a single-pole leaky lens antenna coupled KID operating in a $1.4 - 2.8$ THz frequency band. The device combines excellent sensitivity with a measured optical NEP $= 2.5 \times 10^{-19}$ W/Hz$^{1/2}$ and shows a very good match between the measured and calculated optical coupling efficiency, beam pattern, and frequency response. The efficiency of the measured device is limited by the design choices described in this paper for easier fabrication and assembly. It is possible to increase the efficiency of the device by: (i) The utilisation of a non-antireflective coated lens to reduce reflection loss; (ii) the implementation of a dual thick-thin Al layers to confine the quasiparticles to the

narrow central line of the KID[9] to reduce the loss in the ground plane; (iii) the use of e-beam lithography to reduce the radiation loss in the CPW KID and the impedance mismatch between the KID and the antenna; and (iv) improve the alignment between the lens and the antenna. We expect to achieve an aperture efficiency $\eta_{ap} = 0.66$ for an optimised device. This device and assembly can also be scaled and used for the higher frequency bands (up to 10 THz) of SPICA-SARI.[1] The CPW section of the KID close to the antenna needs to be made with electron beam lithography in order to make $\sim$300 nm lines and the gap between the lens and the antenna needs to be reduced down to 1 μm. This is a serious engineering challenge, but there is no physical reason why it should be achieved.

[1]P. Roelfsema, M. Giard, F. Najarro, K. Wafelbakker, W. Jellema, B. Jackson, B. Swinyard, M. Audard, Y. Doi, M. Griffin, F. Helmich, F. Kerschbaum, M. Meyer, D. Naylor, H. Nielsen, G. Olofsson, A. Poglitsch, L. Spinoglio, B. Vandenbussche, K. Isaak, and J. R. Goicoechea, Proc. SPIE **8442**, 84420R (2012).
[2]C. M. Bradford, M. Kenyon, W. Holmes, J. Bock, and T. Koch, Proc. SPIE **7020**, 70201O (2008).
[3]P. K. Day, H. G. LeDuc, B. A. Mazin, A. Vayonakis, and J. Zmudzinas, Nature **425**, 817 (2003).
[4]J. van Rantwijk, M. Grim, D. van Loon, S. Yates, A. Baryshev, and J. J. A. Baselmans, IEEE Trans. Microwave Theory Tech. **64**, 1876 (2016).
[5]J. J. A. Baselmans, J. Bueno, S. J. C. Yates, O. Yurduseven, N. Llombart, K. Karatsu, A. M. Baryshev, L. Ferrari, A. Endo, D. J. Thoen, P. J. de Visser, R. M. J. Janssen, V. Murugesan, E. F. C. Driessen, G. Coiffard, J. Martin-Pintado, P. Hargrave, and M. Griffin, Astron. Astrophys. **601**, A89 (2017); e-print arXiv:org/abs/1609.01952.
[6]S. Doyle, P. Mauskopf, J. Naylon, A. Porch, and C. Duncombe, J. Low Temp. Phys. **151**, 530 (2008).

[7] P. K. Day, H. G. Leduc, A. Goldin, T. Vayonakis, B. A. Mazin, S. Kumar, J. Gao, and J. Zmuidzinas, Nucl. Instrum. Methods Phys. Res., Sect. A **559**, 561 (2006).

[8] H. McCarrick, D. Flanigan, G. Jones, B. R. Johnson, P. Ade, D. Araujo, K. Bradford, R. Cantor, G. Che, P. K. Day, S. Doyle, H. Leduc, M. Limon, V. Luu, P. D. Mauskopf, A. Miller, T. Mroczkowski, C. Tucker, and J. Zmuidzinas, Rev. Sci. Instrum. **85**, 123117 (2014).

[9] P. J. de Visser, J. J. A. Baselmans, J. Bueno, N. Llombart, and T. M. Klapwijk, Nat. Commun. **5**, 3130 (2014).

[10] J. Hubmayr, J. Beall, D. Becker, H.-M. Cho, M. Devlin, B. Dober, C. Groppi, G. C. Hilton, K. D. Irwin, D. Li, P. Mauskopf, D. P. Pappas, J. van Lanen, M. R. Vissers, Y. Wang, L.-F. Wei, and J. Gao, Appl. Phys. Lett. **106**, 073505 (2015).

[11] L. Ferrari, O. Yurduseven, N. Llombart, S. J. C. Yates, J. Bueno, V. Murugesan, D. J. Thoen, A. M. Baryshev, and J. J. A. Baselmans, "Antenna coupled MKID performance verification for large format astrophysics arrays," IEEE Trans. Terahertz Sci. Technol. (submitted).

[12] M. Griffin, J. Baselmans, A. Baryshev, S. Doyle, M. Grim, P. Hargrave, T. Klapwijk, J. Martin-Pintado, A. Monfardini, A. Neto, H. Steenbeek, I. Walker, K. Wood, A. D'Addabbo, P. Barry, A. Bideaud, B. Blázquez, J. Bueno, M. Calvo, J.-L. Costa-Kramer, L. Ferrari, A. Gómez-Gutiérrez, J. Goupy, N. Llombart, and S. Yates, Proc. SPIE **9914**, 991407 (2016).

[13] J. Dyson, IEEE Trans. Antennas Propag. **7**, 329 (1959).

[14] R. H. DuHamel, U.S. patent application 4,658,262 (1987).

[15] A. Neto, IEEE Trans. Antennas Propag. **58**, 2238 (2010).

[16] O. Yurduseven, N. Llombart, and A. Neto, IEEE Trans. Antennas Propag. **64**, 3330 (2016).

[17] A. Garufo, N. Llombart, and A. Neto, IEEE Trans. Antennas Propag. **64**, 4168 (2016).

[18] R. O'Brient, P. A. R. Ade, K. Arnold, J. Edwards, G. Engargiola, W. L. Holzapfel, A. T. Lee, M. J. Myers, E. Quealy, G. Rebeiz, P. Richards, and A. Suzuki, Appl. Phys. Lett. **102**, 063506 (2013).

[19] A. Neto, N. Llombart, J. J. A. Baselmans, A. M. Baryshev, and S. J. C. Yates, IEEE Trans. Terahertz Sci. Technol. **4**, 26 (2014).

[20] R. M. J. Janssen, J. J. A. Baselmans, A. Endo, L. Ferrari, S. J. C. Yates, A. M. Baryshev, and T. M. Klapwijk, Appl. Phys. Lett. **103**, 203503 (2013).

[21] J. M. Martinis, K. B. Cooper, R. McDermott, M. Steffen, M. Ansmann, K. D. Osborn, K. Cicak, S. Oh, D. P. Pappas, R. W. Simmonds, and C. C. Yu, Phys. Rev. Lett. **95**, 210503 (2005).

[22] R. Barends, H. L. Hortensius, T. Zijlstra, J. J. A. Baselmans, S. J. C. Yates, J. R. Gao, and T. M. Klapwijk, IEEE Trans. Appl. Supercond. **19**, 936 (2009).

[23] J. Gao, M. Daal, J. M. Martinis, A. Vayonakis, J. Zmuidzinas, B. Sadoulet, B. A. Mazin, P. K. Day, and H. G. Leduc, Appl. Phys. Lett. **92**, 212504 (2008).

[24] S. J. C. Yates, J. J. A. Baselmans, A. M. Baryshev, S. Doyle, A. Endo, L. Ferrari, S. Hochgürtel, and B. Klein, J. Low Temp. Phys. **176**, 761 (2014).

[25] TechniEtch Al80 Al etchant from Microchemicals GmbH.

[26] SC-2 clean: H_2O_2 - HCl - H_2O (1:1:5) at 75 °C for 10 min.

[27] See http://www.veldlaser.nl/english/ for Veld Laser Innovations B.V.

[28] B. A. Mazin, "Microwave kinetic inductance detectors," Ph.D. dissertation (California Institute of Technology, 2005).